Conference Paper, Published Version

Kranenborg, Joost; Campmans, Geert; van der Werf, Jebbe; Reniers, Ad; Hulscher, Suzanne

Depth-Resolving vs Depth-Averaged Modelling of Swash Zone Hydrodynamics

Coastal Structures 2019 - Nils Goseberg, Torsten Schlurmann (eds) - © 2019 Bundesanstalt für Wasserbau
ISBN 978-3-939230-64-9 (Online) - DOI: 10.18451/978-3-939230-64-9_083

Depth-Resolving vs Depth-Averaged Modelling of Swash Zone Hydrodynamics

J. Kranenborg[1], G. Campmans[1], J. van der Werf[1,2], A. Reniers[3] & S. Hulscher[1]
[1]*University of Twente, Enschede, The Netherlands*
[2]*Deltares, Delft, The Netherlands*
[3]*Delft University of Technology, Delft, The Netherlands*

Abstract: Numerical models have played a big role in gaining new understanding of processes in the swash zone. Until recently, intra-wave sediment transport and morphology has almost exclusively been studied by depth-averaged models and rarely by depth-resolving models. In this paper we highlight some of the important differences between these model types with respect to their application in the swash zone. We compare the depth-resolving OpenFOAM model with the depth-averaged XBeach nonhydrostatic model when applied to a dambreak case. The models reproduce the overall dynamics of the swash event but tend to overpredict the swash depths and velocities. We also find that the depth-resolving model produces large vertical variation in flow velocity. Depth-averaged models cannot reproduce these vertical variabilities. For this reason, the models differ in their treatment of breaking waves. This leads to differences in the uprush, while the backwash flows are more similar. We conclude that depth-resolving models are an important tool to study the swash flows and potentially sediment transport and morphology.

Swash zone, numerical modelling, hydrodynamics, CFD, breaking waves, turbulence

1 Introduction

The swash zone is the dynamic region between the continuously submerged surf zone and the exposed beachface. In this zone, the strong hydrodynamic forces lead to large sediment fluxes. These sediment fluxes lead to large morphological change, which can be on the order of cm's in seconds (van der Zanden et al., 2015). This dynamic environment still poses a challenge for models in engineering practice, which have difficulty predicting the nearshore morphodynamics (Van Rijn et al., 2011). These models have a wave-averaged framework and thus cannot resolve the swash motion explicitly. The Shaping The Beach research project aims to develop a new parametrization for sediment transport to be used in this type of model. This is done through large-scale wave flume experiments and detailed numerical modelling (see the Coastal Structures paper by van der Werf et al. (2019) for further details on the project). In this paper the detailed numerical modelling is introduced.

Experimental studies provide a good opportunity to study the swash zone. There have been numerous studies on natural beaches, but it is difficult to measure the small-scale processes in uncontrolled, natural conditions (Masselink & Puleo, 2006). Laboratory experiments have given tremendous insight in swash processes such as turbulence, bed shear stress, sediment transport rates, pressure gradients and wave-swash interactions. However, it is difficult to single out specific processes and instrumental coverage is generally restricted to specific points only. This is one of the reasons why wave-resolving numerical models can complement experiments.

Numerical models for the swash zone can generally be divided into two classes. The more detailed models include the vertical direction in their solution and are thus called depth-resolving models. Conversely, depth-averaged models do not resolve the vertical direction. These two different model types have different strengths and weaknesses. Depth-resolving models do not need to assume a certain vertical structure in the flow and thus can solve the flow field more completely. On the other

hand, these models are computationally expensive. Depth-averaged models do need to make assumptions on the vertical structure of the flow. However, this makes them less computationally demanding. These different strengths and weaknesses mean that the models have been applied to different problems.

Depth-resolving models have previously been used to study small-scale processes on shorter timescales, primarily considering swash hydrodynamics. Previous studies have focused on how the bed shear stress behaves (Torres-Freyermuth et al., 2013), how infiltration/exfiltration affects the swash volume and the boundary layer (Pintado-Patiño et al., 2015), turbulent structures under breaking waves (Zhou et al., 2017) and detailed flow structure and vortices (Higuera et al., 2018). Depth-averaged models have typically been used to study a broad range of phenomena, also on longer timescales and including sediment transport and morphology. Examples of previous studies involve turbulence effects on sediment transport and grain size variability (Reniers et al., 2013) or groundwater interactions and their effect on sediment transport (McCall et al., 2015).

In this paper we aim to make clear the fundamental differences between these model types in how they handle hydrodynamics by means of a model-to-model comparison and comparing with experimental data. In Section 2 the two models and the study case are introduced. In Section 3 the results are presented which are discussed in section 4. Finally, Section 5 outlines the most important conclusions and provides an outlook for the future development of the models.

2 Model and case setup

2.1 Dambreak case description

We use the fixed-bed dambreak experiments by O'Donoghue et al., (2010) as a testcase. Specifically, we use the results from the smooth-bed experiments, where the bed consisted of Perspex panels. The experiments release a water reservoir by quickly raising a gate. The water depth in the reservoir is 0.65m and the water depth is 0.06m in the flume (Fig. 1). The reservoir is 1m long and is followed by a 4m long region of shallow water with a straight bed level. The release of the reservoir produces a bore which moves towards and onto a fixed plate with a slope of 1:10. For both models, the initial conditions were the same as in the experiments excluding the gate motion. Instead, the water is released instantaneously when the simulation starts.

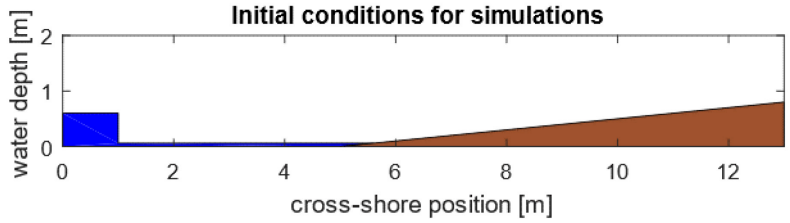

Fig. 1. Schematic overview of the model initial conditions. Here blue is the initial position of the water and brown denotes the fixed bed.

The experimental data consists of ensemble-averaged run-up, swash depths and velocity profile measurements over 50 swash repetitions. The run-up and depths were measured using capacitance depth-gauges at 25 cross-shore locations at 100 Hz. The velocity profile measurements were taking using particle image velocimetry (PIV) at six cross-shore locations at 13 Hz.

2.2 Depth-resolving model: OpenFOAM

For the depth-resolving model, we use the open-source toolbox OpenFOAM® for CFD applications. In this case we use the Reynolds Averaged Navier-Stokes (RANS) equations for the fluid momentum coupled with a k-ε turbulence closure (El Tahry, 1983) and a Volume of Fluid (VOF) scheme to capture the air/water interface. The model distinguishes between water and air using an α parameter, where α=1 means a cell contains only water and α=0 means a cell contains only air. The equations are discretized using the finite volume method.

The OpenFOAM model uses a grid resolution of 0.5x0.5cm throughout the whole domain, which spans 2600 cells in the cross-shore direction and 160 cells in the depth direction for our case-study. This is sufficient to give an impression of the large scale 2DV motions in the swash, but this is too coarse to capture the bottom boundary layer processes. At the bottom, a no-slip condition is imposed on the velocity and logarithmic velocity profile for a smooth wall is assumed. At time t=0 the air and water are assumed to be turbulence free. Furthermore, the time discretization is adaptive such that the maximum Courant number (defined for every grid cell as $C=\Delta t\ \Sigma(u_i/\Delta x_i)$ where Δt and Δx_i are the timestep length and the cell width respectively, u_i is the cell velocity and the index i denotes the spatial dimension) is less than 0.5.

2.3 Depth-averaged model: XBeach

For the depth-averaged model, we use the non-hydrostatic version of the open-source XBeach model. This model uses the depth-averaged Nonlinear Shallow-water Equations (NSWE) with a nonhydrostatic-pressure correction to solve the depth-averaged wave quantities (see Smit, et al. (2014) for details on the model implementation). Contrary to the OpenFOAM model, we do not include a transport equation for turbulence, however an eddy viscosity based on a Smagorinsky-type model is included. The bed shear stress τ due to friction is modelled as $\tau = 0.5C_f\rho|u|u$, where $C_f = 0.002$ (extrapolated after O'Donoghue et al., (2010)), ρ is the water density and u denotes the depth-averaged velocity. The model cannot reproduce the curling of a wave that occurs during the breaking process, but it includes a procedure to simulate the effect of wave breaking on energy dissipation (Smit et al., 2013). The XBeach model was run on a grid resolution of 1cm, resulting in 1300 grid points. The adaptive timestep was such that the Courant number stayed below 0.1.

3 Results

These results are produced by simulating 15 seconds and are computed on a 3.7GHz Intel Xeon 8 core processor. The OpenFOAM simulation was done in parallel on four cores while the XBeach simulation was done serially on one core. The computational time for the OpenFOAM simulation was 10 hours in wall clock time. XBeach took 33 seconds for the simulation.

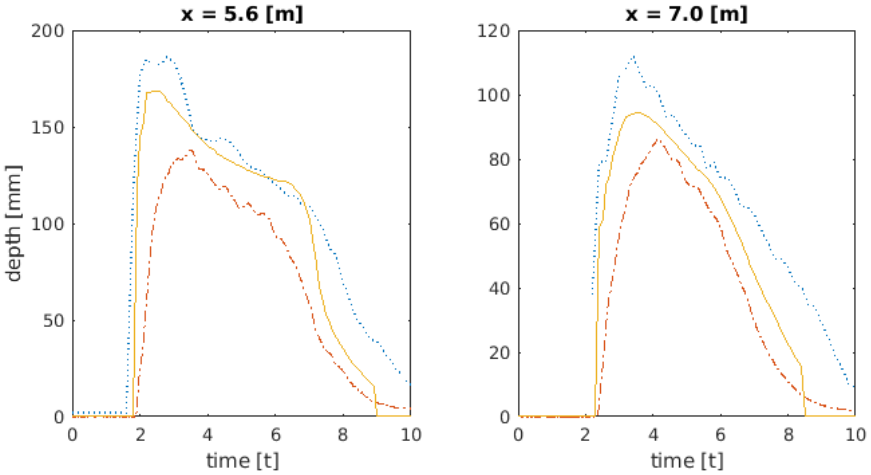

Fig. 2. Comparison between swash depths from experimental data (red dash-dotted line), OpenFOAM (blue dotted line) and XBeach (yellow line) at two cross-shore locations.

3.1 Surface elevation

First, we compare the model results with the experimental results (Figure 2). From XBeach we retrieve the water depth directly. From OpenFOAM the water surface is assumed to be at the topmost position where $\alpha = 0.5$. Both models and the experiments show a steep front when the swash arrives the measurement location. During the backwash the water depth fall more slowly, which is also captured by the models. However, both models predict a larger swash volume compared to the data.

In Figure 3 we compare the two models at four different swash stages. At t=0s, the reservoir collapses and generates a bore. After one second the bore is propagating through the flat region of the flume. In OpenFOAM the shape of the bore and the air content in the water is clearly visible. In XBeach the bore propagation is also clearly visible but since the shallow water equations cannot reproduce the curling wave shape the bore is modelled as a steep surface gradient. Also, the solution does not include the air. After two seconds the bore has reached the sloping beach in both solutions. In the OpenFOAM model pockets of air still exist in the bore front. Also, at approximately x=2.6m a wave has emerged that moves to the left. The bore front in the XBeach solution has flattened considerably compared to the very steep front at t=1 s. After approximately five seconds the point of highest runup is reached by both models. At x=4m a bore has formed in both models that moves to the left. Finally, after nine seconds the backwash phase is almost over. At approximately x=5m the interaction between the fast-flowing backwash and the slower water leads to the formation of a bore. In OpenFOAM this bore is seen by the steep water surface. In XBeach the interactions lead to strong oscillations.

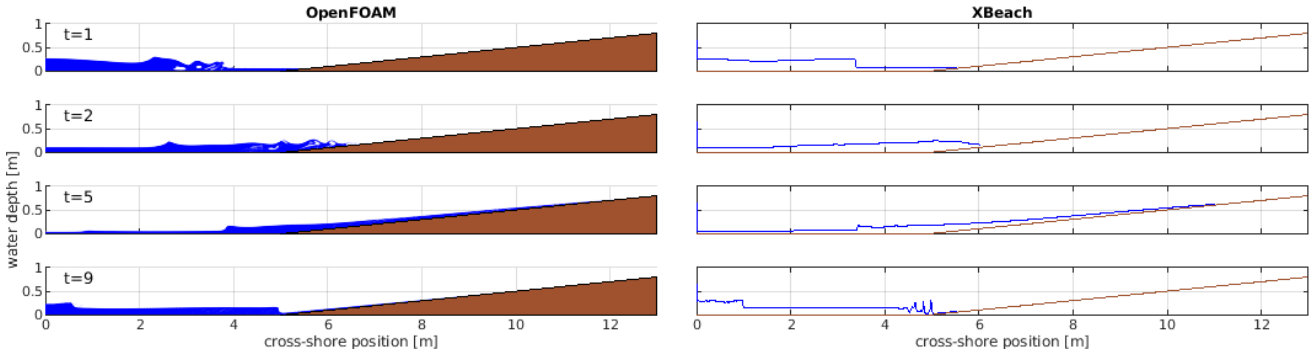

Fig. 3. Comparison between the solutions of OpenFOAM and XBeach of the water column for a dam-break swash event. Note that the OpenFOAM solution is a function of both depth and cross-shore position while the XBeach solution is only a function of the cross-shore position.

3.2 OpenFOAM flow characteristics

In Figure 4 vertical velocity profiles from the OpenFOAM model and the experiments are compared. During earlier stages in the swash the model produces similar data compared with the experiments. However, during the latter stages the model lags behind the data.

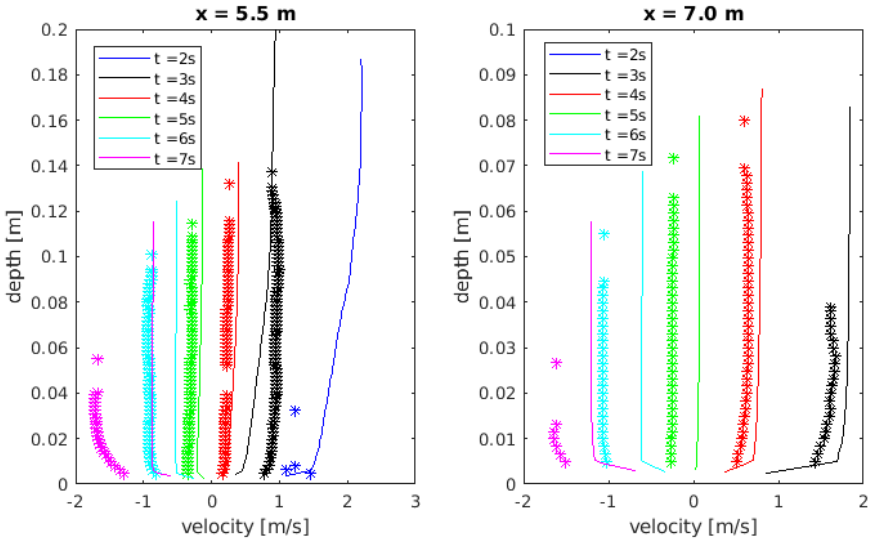

Fig. 4. Comparison of depth-dependent bed-parallel velocity profiles at two cross-shore locations. The crosses show the ensemble averaged PIV measurements and the lines show the OpenFOAM model results. The data agrees better during earlier stages than latter stages of the swash.

Using depth-resolving models we can get an insight in how vertical features of the flow behave. This is shown in figure 5 where two snapshots of the swash can be seen. The first at t=2 s shows the bore arriving at the beach. The second at t=5 shows the lower swash around the transition from uprush to

backwash. The uprush is characterized by localized patches of high velocity and turbulence. The velocity peaks reach well over 2 m/s and are localized near the swash tip. It is also evident that the velocity varies strongly in the vertical direction. Patches of high turbulent kinetic energy are concentrated around the swash tip and the velocity peaks. Around the transition to backwash the localized high velocity and turbulent kinetic energy patches have dispersed into the water column. At the lower parts of the beach (approx. x = 4m) a backwards traveling bore has formed.

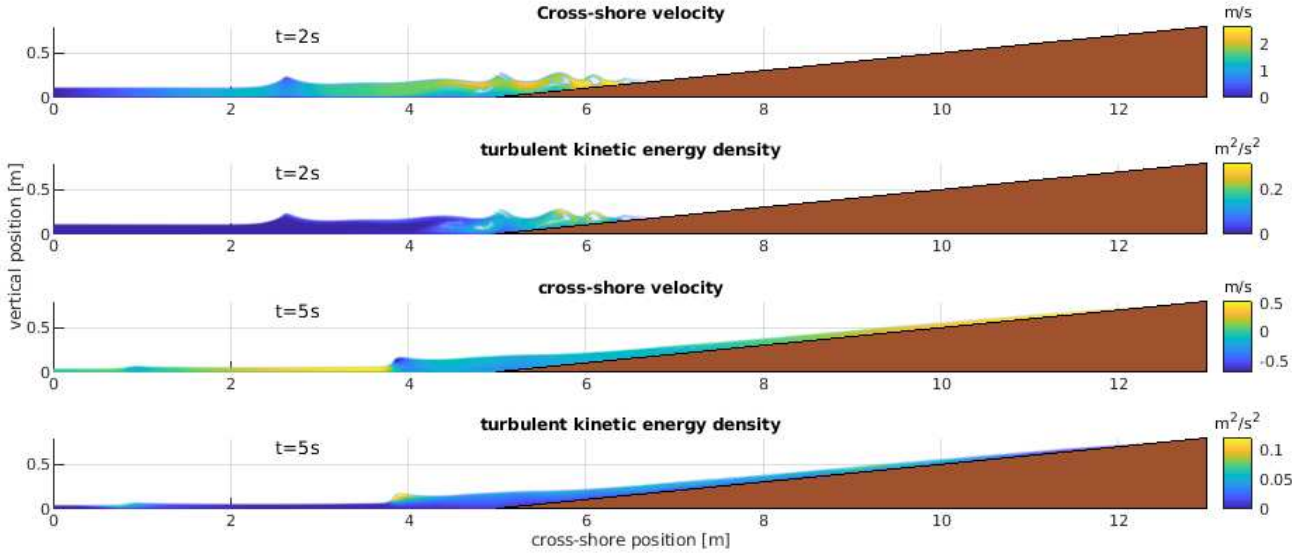

Fig. 5. Results from OpenFOAM on the cross-shore velocity [m/s] and turbulent kinetic energy density [m^2/s^2]. The top two figures show the turbulent bore reaching the beach after two seconds. The bottom two plots show the transition from uprush to backwash happening after five seconds. In all four figures only the results for the water phase are shown.

3.3 XBeach flow characteristics

For validation of XBeach we use depth-averaged velocity measurements instead (Fig. 6). XBeach captures the overall characteristics of the swash motion. The arrival of the bore at the measurement locations leads to a sharp gradient in the velocity, which is slightly overpredicted by XBeach. During a large timespan the XBeach results agree well with the experimental data. However, at the end of the backwash the velocity and backwash duration are overpredicted.

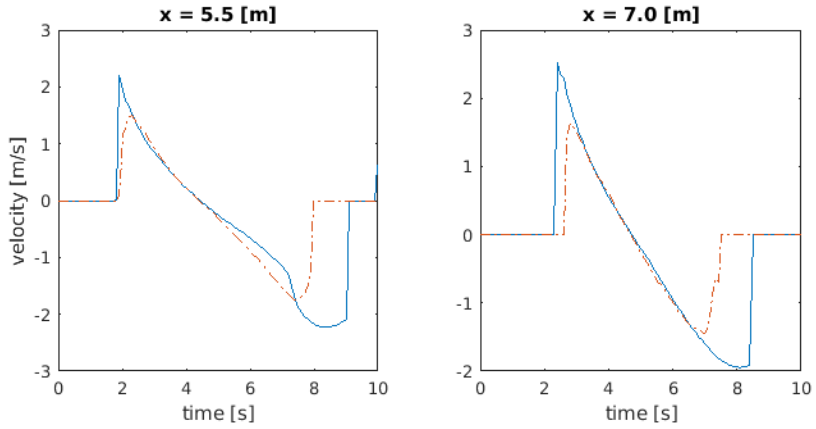

Fig. 6. Comparison of depth-averaged bed-parallel velocities between XBeach (blue line) and model data (dash-dotted red line) at two cross-shore locations. Apart from the latter stages in the backwash and the sharp spike at bore arrival, the model data lines up with the experimental data. However, XBeach produces erroneous results at the end of the backwash.

In Figure 7 the flow velocities and regions of wave breaking can be seen for two different stages of the swash motion. At t=2 s, the highest flow velocities are, similar as in the OpenFOAM simulation, concentrated at the swash tip. XBeach also predicts wave breaking at the swash tip. After five seconds

the transition from uprush to backwash is clearly visible. Also, again a backwards traveling bore is formed by the model.

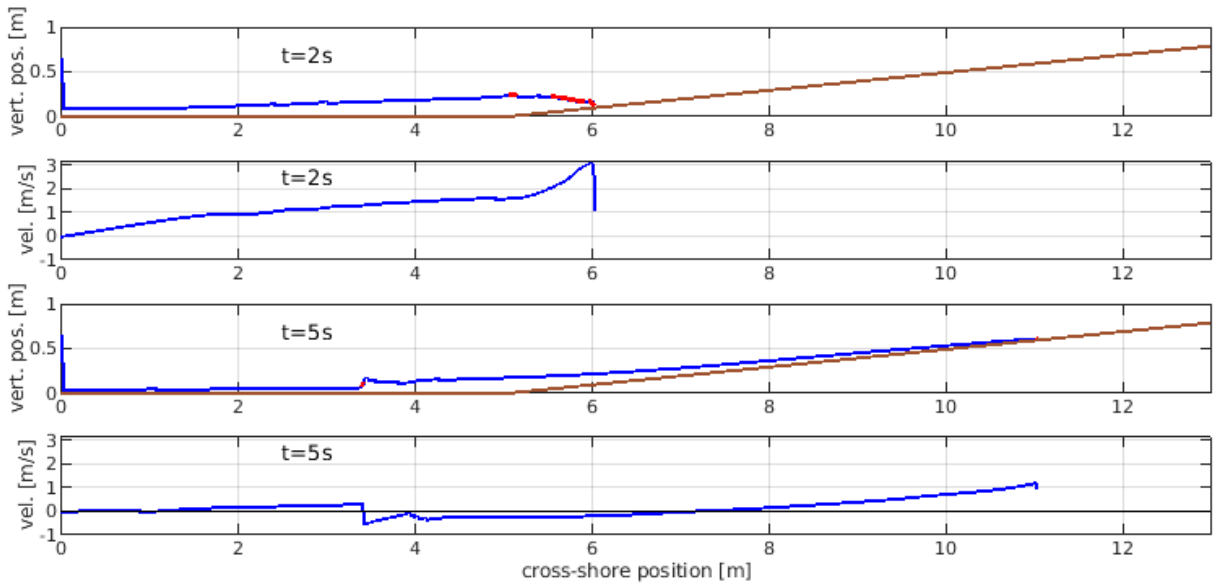

Fig. 7. Results from the XBeach simulation showing the flow velocities and water surface elevation. The red regions show where XBeach applies the wave breaking procedure. The values are not plotted where the beachface is exposed.

4 Discussion

When compared with the data, both models (i.e. XBeach and OpenFoam) overpredict the swash volume, leading to longer swash events compared to the experiment. The differences could be explained by how the bed friction was included in the models. The present study assumes a smooth bed. However, Torres-Freyermuth et al. (2013), who used a similar RANS model on the same case, assumed bed friction similar to sand grains with a diameter of 0.2 mm. Their result match the data better, indicating that the smooth wall assumption needs to be improved upon. The XBeach results could be explained similarly. O'Donoghue et al. (2010) showed that the friction factor lies around $0.002<C_f<0.005$. Masselink and Hughes (1998) have previously shown that the friction factor during uprush is roughly twice as large as during the backwash. This effect is not incorporated here and could also lead to a decrease in the modelled swash volume. Apart from this, other factors can be improved such as the choice of turbulence model or grid. Still with these areas of improvement in mind, the models both capture much of the dynamics in the swash.

Qualitatively the models produce similar results in terms of surface elevation and the cross-shore velocity. During uprush both models produce cross-shore velocities of up to 3 m/s at the swash tip. At the transition from uprush to backwash, both models show horizontal velocity profiles where the swash tip still moves shoreward while the lower swash moves seaward. In Figure 7 the vertically varying flow structures around the breaking bore are clearly visible. Since XBeach cannot resolve these vertical structures it produces a different surface profile at the tip of the swash. Similarly, XBeach has difficulty with the backwash bore and produces large oscillations (Fig. 3).

Since the models are based on different equations, they deal differently with the process of wave breaking. Figure 3 shows the strength of depth-resolving models in their capability to resolve more complex flow patterns and air entrainment in the water column. Figure 7 shows that XBeach predicts wave-breaking to happen both at the swash tip during uprush and at the bore generated at the backwash. Interestingly, these are the same regions where OpenFOAM predicts large amounts of turbulence. This can be seen both at t=2s at the swash tip and at t=5s at the backwash bore front.

5 Conclusion and outlook

Both depth-resolving models and depth-averaged models are powerful tools but do present different solutions and challenges. Depth-averaged models benefit from their lower computational cost. This makes them very suitable for studying longer-term processes on the scale of days. However, vertical effects in the flow need to be parametrized. Depth-resolving models can potentially give insight in these vertical structures but are computationally more expensive and complex. Their complexity also means one needs to take care in choosing appropriate turbulence and boundary layer models.

This paper highlights differences in how two specific models, the OpenFoam and XBeach model, treat hydrodynamics, but both models have been used to study sediment transport and morphodynamics as well, even though depth-resolving model applications to the swash are rare. Only recently did Li et al. (2019) use a fully coupled depth-resolving model to simulate the bed response to a solitary wave. However, depth-resolving morphodynamic models have yet to be used to study the vertical structures affecting sediment transport. Further investigations of swash zone morphodynamics using depth-resolving models will give new insights in the processes behind sediment transport and morphodynamics. These insights can then be used improve parametrizations for sediment transport for use in other models.

Acknowledgements

This paper is produced as part of the Shaping The Beach project. Shaping The Beach (2018-2023) is an NWO-TTW funded research project (no. 16130), with in-kind support by Deltares. We would like to thank Niels Jacobsen and Robert McCall for the fruitful discussions.

References

El Tahry, S. (1983). k-epsilon equation for compressible reciprocating engine flows. *Journal of Energy*, 345-353.

Higuera, P., Liu, P. L.-F., Lin, C., Wong, W.-Y., & Kao, M.-J. (2018). Laboratory-scale swash flows generated by a non-breaking solitary wave on a steep slope. *Journal of Fluid Mechanics*, *847*, 186–227. https://doi.org/10.1017/jfm.2018.321

Li, J., Qi, M., & Fuhrman, D. R. (2019). Numerical modeling of flow and morphology induced by a solitary wave on a sloping beach. *Applied Ocean Research*, *82*(November 2018), 259–273. https://doi.org/10.1016/j.apor.2018.11.007

Masselink, G., & Puleo, J. A. (2006). Swash-zone morphodynamics. *Continental Shelf Research*, *26*(5), 661–680. https://doi.org/10.1016/j.csr.2006.01.015

Masselink, G. & Hughes, M. (1998). Field investigation of sediment transport in the swash zone. Continental Shelf Research, 18 (10), 1179 -1199.

McCall, R. T., Masselink, G., Poate, T. G., Roelvink, J. A., & Almeida, L. P. (2015). Modelling the morphodynamics of gravel beaches during storms with XBeach-G. *Coastal Engineering*, *103*, 52–66. https://doi.org/10.1016/j.coastaleng.2015.06.002

O'Donoghue, T., Pokrajac, D., & Hondebrink, L. J. (2010). Laboratory and numerical study of dambreak-generated swash on impermeable slopes. *Coastal Engineering*, *57*(5), 513–530. https://doi.org/10.1016/j.coastaleng.2009.12.007

Pintado-Patiño, J. C., Torres-Freyermuth, A., Puleo, J. A., & Pokrajac, D. (2015). On the role of infiltration and exfiltration in swash zone boundary layer dynamics. *Journal of Geophysical Research: Oceans*, 6329-6350.

Reniers, A. J. H. M., Gallagher, E. L., MacMahan, J. H., Brown, J. A., Van Rooijen, A. A., Van Thiel De Vries, J. S. M., & Van Prooijen, B. C. (2013). Observations and modeling of steep-beach grain-size variability. *Journal of Geophysical Research: Oceans*, *118*(2), 577–591. https://doi.org/10.1029/2012JC008073

Smit, P., Zijlema, M., & Stelling, G. (2013). Depth-induced wave breaking in a non-hydrostatic, near-shore wave model. *Coastal Engineering*, *76*, 1–16. https://doi.org/10.1016/j.coastaleng.2013.01.008

Smit, P., G.S.Stelling, Roelvink, D., Vries, J. v., R. McCall, A. v., Zwinkels, C., & Jacobs, R. (2014). *XBeach: Non-hydrostatic model.*

Torres-Freyermuth, A., Puleo, J. A., & Pokrajac, D. (2013). Modeling swash-zone hydrodynamics and shear stresses on planar slopes using Reynolds-Averaged Navier-Stokes equations. *Journal of Geophysical Research: Oceans*, *118*(2), 1019–1033. https://doi.org/10.1002/jgrc.20074

van der Zanden, J., Alsina, J. M., Cáceres, I., Buijsrogge, R. H., & Ribberink, J. S. (2015). Bed level motions and sheet flow processes in the swash zone: Observations with a new conductivity-based concentration measuring technique (CCM+). *Coastal Engineering*, *105*, 47–65. https://doi.org/10.1016/j.coastaleng.2015.08.009

Van Rijn, L. C., Tonnon, P. K., & Walstra, D. J. R. (2011). Numerical modelling of erosion and accretion of plane sloping beaches at different scales. *Coastal Engineering*, *58*(7), 637–655. https://doi.org/10.1016/j.coastaleng.2011.01.009

Zhou, Z., Hsu, T.-J., Cox, D., & Liu, X. (2017). Large-eddy simulation of wave-breaking induced turbulent coherent structures and suspended sediment transport on a barred beach. *Journal of Geophysical Research: Oceans*, 207-235.